



Article

Epidermal Fatty Acid-Binding Protein 5 (FABP5) Involvement in Alpha-Synuclein-Induced Mitochondrial Injury under Oxidative Stress

Yifei Wang , Yasuharu Shinoda , An Cheng , Ichiro Kawahata and Kohji Fukunaga *

Department of Pharmacology, Graduate School of Pharmaceutical Sciences, Tohoku University, 6-3 Aramaki-Aoba, Aoba-ku, Sendai 980-8578, Japan; yifei.wang.q4@dc.tohoku.ac.jp (Y.W.); yshinoda@tohoku.ac.jp (Y.S.); cheng.an.q6@dc.tohoku.ac.jp (A.C.); kawahata@tohoku.ac.jp (I.K.)

* Correspondence: kfukunaga@tohoku.ac.jp; Tel.: +81-22-795-6836

Abstract: The accumulation of α -synuclein (α Syn) has been implicated as a causal factor in the pathogenesis of Parkinson's disease (PD). There is growing evidence that supports mitochondrial dysfunction as a potential primary cause of dopaminergic neuronal death in PD. Here, we focused on reciprocal interactions between α Syn aggregation and mitochondrial injury induced by oxidative stress. We further investigated whether epidermal fatty acid-binding protein 5 (FABP5) is related to α Syn oligomerization/aggregation and subsequent disturbances in mitochondrial function in neuronal cells. In the presence of rotenone, a mitochondrial respiratory chain complex I inhibitor, co-expression of FABP5 with α Syn significantly decreased the viability of Neuro-2A cells compared to that of α Syn alone. Under these conditions, FABP5 co-localized with α Syn in the mitochondria, thereby reducing mitochondrial membrane potential. Furthermore, we confirmed that pharmacological inhibition of FABP5 by its ligand prevented α Syn accumulation in mitochondria, which led to cell death rescue. These results suggested that FABP5 is crucial for mitochondrial dysfunction related to α Syn oligomerization/aggregation in the mitochondria induced by oxidative stress in neurons.

Keywords: α -Synuclein; FABP5; aggregation; mitochondria; Parkinson's disease



Citation: Wang, Y.; Shinoda, Y.; Cheng, A.; Kawahata, I.; Fukunaga, K. Epidermal Fatty Acid-Binding Protein 5 (FABP5) Involvement in Alpha-Synuclein-Induced Mitochondrial Injury under Oxidative Stress. *Biomedicines* **2021**, *9*, 110. <https://doi.org/10.3390/biomedicines9020110>

Received: 28 December 2020

Accepted: 20 January 2021

Published: 22 January 2021

Publisher's Note: MDPI stays neutral with regard to jurisdictional claims in published maps and institutional affiliations.



Copyright: © 2021 by the authors. Licensee MDPI, Basel, Switzerland. This article is an open access article distributed under the terms and conditions of the Creative Commons Attribution (CC BY) license (<https://creativecommons.org/licenses/by/4.0/>).

1. Introduction

Parkinson's disease (PD) is the second-most common neurodegenerative disease, and is caused by the loss of dopaminergic neurons in the substantia nigra pars compacta (SNpc) [1]. The neuropathological hallmark of PD is the accumulation of intracellular protein inclusions composed primarily of α -synuclein (α Syn), which are termed Lewy bodies [2,3]. Moreover, α Syn aggregation has been widely reported to be a harbinger of subsequent pathology that ultimately leads to neurodegeneration [4]. α Syn is expressed pre-synaptically as a native unfolded protein that can form oligomers, protofibrils, or amyloid fibrils [5,6]. Among the different species of α Syn, pre-fibrillar oligomers are considered to be toxic to neurons [7]. The development of treatments aimed at reducing α Syn synthesis, secretion, aggregation, and increasing the clearance of pathogenic formations has become the most promising means to overcome Parkinson's disease [8,9].

Several lines of evidence support mitochondrial dysfunction as a primary pathogenic mechanism in PD. The most convincing evidence first appeared from accidental human exposure to 1-methyl-4-phenyl-1,2,3,6-tetrahydropyridine, a metabolite that induces Parkinsonian syndrome by inhibiting mitochondrial respiratory complex I activity [10,11]. The genetic causes of PD, including *PINK1*, *parkin*, and *DJ-1*, particularly highlight the importance of mitochondrial dysfunction in PD pathology [12]. Accumulating studies have demonstrated that α Syn itself is involved in mitochondrial injury in PD [13–15]. In postmortem brains of PD patients, α Syn is especially localized to mitochondrial outer membranes in nigrostriatal neurons, which was replicated in rodents treated with rotenone, a

respiratory chain complex I inhibitor [14]. Treatment of α Syn oligomers, but not monomers, disturbed mitochondrial maintenance, leading to fission, reduction in mitochondrial membrane potential, and upregulation of reactive oxidative stress in neuroblastoma cells. Preformed fibril treatment also elicited the translocation of phosphorylated α Syn aggregates to mitochondria, resulting in increased oxidative stress and mitochondrial dysfunction in mouse primary hippocampal neurons [13]. These results indicate the bilateral links that oligomeric α Syn localization in mitochondria induces reactive oxidative species production/mitochondrial dysfunction, and vice versa.

Fatty acid-binding proteins (FABPs) are a set of 14–15 kDa cytoplasmic proteins that are traditionally considered as lipid chaperones that coordinate lipid responses inside cells. FABPs perform pleiotropic functions to maintain healthy tissue homeostasis, and participate in the pathogenesis of diseases [16]. To date, at least 10 genes encoding FABPs (*FABP1-9* and *FABP12*) have been identified in the human genome [17,18]. FABP5 localizes to the cytosol, mitochondria, and nucleus, suggesting a role for fatty acid metabolism and nuclear transcriptional regulation [19,20]. The central nervous system contains three types of FABP, that is, epidermal FABP (E-FABP, FABP5), heart FABP (H-FABP, FABP3), and brain FABP (B-FABP, FABP7) [21]. FABP5 is expressed in neurons and glial cells in broad areas of the brain, including the cortex, hippocampus, and caudate putamen [22]. Moreover, it has been reported that *FABP5* mRNA expression levels, as well as α Syn and tyrosine hydroxylase gene expression levels, are enriched in dopaminergic neurons of the SNpc, and decrease after 6-hydroxydopamine injection in rats [23]. However, little is known regarding whether FABP5 is involved in α Syn toxicity in dopaminergic neurons, or in the pathogenesis of PD.

To investigate whether FABP5 is related to α Syn oligomerization and mitochondrial impairment, we transfected FABP5 with α Syn into neuroblastoma Neuro-2A cells, and evaluated cell viability, α Syn oligomerization, cellular localization, and mitochondrial membrane potential. Here, we report that FABP5 co-expression with α Syn reduced cell viability, upregulated α Syn oligomerization, and aggregation under oxidative stress. FABP5 and α Syn co-localized in mitochondria in the presence of rotenone, which was abolished by a ligand with high affinity for FABP5.

2. Materials and Methods

2.1. Materials

Reagents and antibodies were obtained from the following sources: anti- α Syn antibody (1:1000; 4B12, GeneTex, Irvine, CA, USA); anti-FABP5 antibody (1:1000; AF3077, R&D Systems, Minneapolis, MN, USA); anti- β -tubulin antibody (1:3000; T0198, Sigma-Aldrich, St Louis, MO, USA); anti-VDAC antibody (1:1000; 4866S, Cell Signaling Technology, Danvers, MA, USA); anti-rabbit or mouse IgG antibody conjugated with horseradish peroxidase (1:5000; Southern Biotech, Birmingham, AL, USA); anti-goat IgG antibody conjugated with peroxidase (1:5000; Rockland Immunochemical, Limerick, PA, USA); Alexa 594-labeled anti-mouse IgG, Alexa 488-labeled anti-Goat IgG and Alexa 594-labeled anti-rabbit IgG antibody (1:500; Invitrogen, Waltham, MA, USA); Biotin-SP anti-Goat IgG antibody (1:500; Jackson ImmunoResearch, West Grove, PA, USA); and AMCA streptavidin (1:500; Jackson ImmunoResearch). These materials were used according to the manufacturers' datasheets. Rotenone was purchased from MP Biomedicals (150154; Santa Ana, CA, USA). All other reagents were obtained from FUJIFILM Wako Pure Chemicals (Osaka, Japan) unless otherwise noted. The FABP5 ligand (ligand 7) was described in a previous report [24].

2.2. Cell Culture and Transfection

Neuro-2A cells were obtained from the Human Science Research Resources Bank (IFO50081) (Osaka, Japan). Cells were maintained in Dulbecco's modified Eagle medium (DMEM) supplemented with 10% fetal bovine serum (FBS) and 100 U/mL penicillin-streptomycin at 37 °C in a humidified atmosphere of 5% CO₂. For stimulation, rotenone and FABP ligands were prepared in dimethyl sulfoxide (DMSO). Mouse FABP5 plasmid

was produced as described previously [24], and inserted into the multiple cloning site of plasmid pcDNA3.1 (Invitrogen). Human α Syn plasmid encoding the protein with myc and 6 \times His tag at the C-terminus was purchased from Abgent (San Diego, CA, USA). A non-coding plasmid (pcDNA3.1) was used for a mock group. Transfection was carried out using Lipofectamine LTX and Plus Reagent (Invitrogen) by incubating for 6 h. The medium was then changed to DMEM supplemented with 5% FBS to maintain cell viability. The next day, cells were treated with rotenone, ligand 7, or DMSO for 48 h at a dilution of 1:1000, and then used for the following experiments.

2.3. Evaluation of Cell Viability

Cells were cultured in 96-well microplates, and 1:10 dilution of CCK-8 solution was added after transfection and drug treatment (Cell Counting Kit-8; Dojindo, Kumamoto, Japan). Plates were incubated for 2 h at 37 °C, and the optical absorbance at 450 nm was measured using a microplate reader (Flex Station 3, Molecular Devices, San Jose, CA, USA).

2.4. Protein Extraction and Immunoblotting Assay

Cells were cultured in a 35 mm dish, collected by scraping, and homogenized in 80 μ L buffer containing 0.5% Triton X-100, 50 mM Tris-HCl, pH 7.4, 4 mM EGTA, 10 mM EDTA, 1 mM Na_3VO_4 , 40 mM $\text{Na}_4\text{P}_2\text{O}_7 \cdot 10\text{H}_2\text{O}$, 50 mM NaF, 0.15 M NaCl, and protease inhibitor cocktail (50 μ g/mL leupeptin, 25 μ g/mL pepstatin A, 50 μ g/mL trypsin inhibitor, 100 nM calyculin A, and 1 mM dithiothreitol). Then, lysates were centrifuged at 15,000 rpm (10,000 \times g) for 10 min at 4 °C, the supernatants (Triton-soluble fraction) collected, and protein concentrations were measured using the Bradford assay. Insoluble materials were washed three times and centrifuged at 15,000 rpm for 3 min at 4 °C, and the supernatant was discarded. The pellets were homogenized in 2% SDS solution (SDS-soluble fraction). In order to ensure equivalent protein loading, the volume of the 2% SDS solution was proportional to the concentration of Triton-soluble protein. Mixtures with Laemmli's sample buffer without β -mercaptoethanol were subjected to heating before immunoblotting to evaluate α Syn oligomerization.

For immunoblotting assays, equal amounts of protein were electrophoresed on ready-made gels (414886; Cosmo Bio, Tokyo, Japan) and transferred onto PVDF membranes (Millipore, Billerica, MA, USA). After blocking with 5% skim milk in Tris-buffered saline with Tween 20, the membrane was incubated on a horizontal shaker overnight with primary antibody at 4 °C, followed by probing with secondary antibody for 2 h at 20 °C. Signals were detected by chemiluminescence using an imaging analyzer (LAS4000 Mini, Fuji Film, Tokyo, Japan). Densitometry analysis was performed using Multi Gauge Software (FUJIFILM). Briefly, we framed each target band and also framed the part without bands as the background to get their densities. The difference between the two is the intensity of the target band and is standardized with the internal reference protein (β -tubulin). Finally, the values were normalized with the mock group before statistical analysis.

2.5. Immunofluorescent Staining

Neuro-2A cells were cultured on glass slips in 12-well plates (Corning, Glendale, AZ, USA) and fixed in 4% paraformaldehyde for 10 min at room temperature. For mitochondrial staining, cells were incubated with 0.1mM MitoTracker Red CMXRos dye (M7512; Invitrogen) in DMEM without FBS for 30 min at 37 °C before fixation. Cells were washed in phosphate-buffered saline (PBS) and permeabilized with 0.1% Triton X-100/PBS for 10 min, then blocked in 1% BSA/PBS at room temperature for 30 min. Cells were incubated with primary antibodies at 4 °C overnight. After washing in 1% BSA/PBS for 5 min three times, cells were incubated with secondary antibodies for 2 h at 4 °C. Cells were washed in 1% BSA/PBS for 5 min three times, followed by staining with 4',6-diamidino-2-phenylindole (DAPI) (Thermo Fisher Scientific, Waltham, MA, USA). Glass slips were mounted with Vectashield (Vector Laboratories, Burlingame, CA, USA). Immunofluorescent images were

captured with a confocal laser scanning microscope (TCS SP8, Leica Microsystems, Wetzlar, Germany). The visible aggregates (diameter 0.5–2 μm approximately) were quantitated.

2.6. Measurement of Mitochondrial Membrane Potential

Cells were cultured in 96-well plates (Corning) or glass-bottom dishes (Matsunami Glass Ind, Osaka, Japan). Mitochondrial activity was visualized using JC-1 MitoMP Detection Kit (Dojindo) staining, according to the manufacturer's instructions. JC-1 is a cationic dye that exhibits membrane potential-dependent accumulation in mitochondria, which is indicated by a fluorescence emission shift from green (~530 nm) to red (~590 nm). The fluorescence intensity was measured with Flex Station 3, or using ImageJ software following acquisition of images by confocal microscopy [25]. The ratio of red/green fluorescence intensity was calculated and converted into a value relative to the control group for the identification of mitochondrial membrane potential.

2.7. Mitochondrial Purification

Mitochondria and cytoplasm were isolated from Neuro-2A cells as described previously [26] with slight modifications. Briefly, cells were suspended in mitochondrial isolation buffer containing 250 mM sucrose, 1 mM dithiothreitol, 10 mM KCl, 1 mM EDTA, 1.5 mM MgCl_2 , protease inhibitors, and 20 mM Tris-HCl, pH 7.4, and then homogenized with a glass homogenizer using approximately 30 strokes, on ice. The homogenate was centrifuged twice at $800\times g$ for 10 min. The supernatant was further centrifuged at $15,000\times g$ for 10 min. After that, supernatants were collected as cytosolic fractions (without mitochondria). Next, the mitochondrial pellets were immediately washed three times in mitochondrial isolation buffer. Subsequently, the pellets were homogenized with Triton X-100 buffer as described above, and supernatants were collected as mitochondrial fractions. All steps were carried out at 4 $^\circ\text{C}$. Protein concentrations were determined by using Bradford assays. All fractions were boiled at 100 $^\circ\text{C}$ for 3 min with six \times Laemmli sample buffer containing β -mercaptoethanol. The quantity of cytosolic fractions and mitochondria were, respectively, estimated by quantification of β -tubulin and VDAC using an immunoblotting assay.

2.8. Statistical Analysis

Values are presented as means \pm standard error of the mean (SEM), and were evaluated with one- or two-way analysis of variance (ANOVA) followed by Bonferroni's multiple comparisons test using GraphPad Prism 7.04 (GraphPad Software, San Diego, CA, USA). $p < 0.05$ was considered statistically significant.

3. Results

3.1. Co-Overexpression of FABP5 and α -Synuclein Increases Neurotoxicity in the Presence of Rotenone

To address the role of FABP5 in the toxicity of α Syn and oxidative stress, Neuro-2A cells were transfected with plasmids and then stimulated with 0.01–10 μM rotenone (Figure 1). Immunoblotting analysis showed moderate levels of endogenous FABP5 protein and higher levels of FABP5 and α Syn in transfected cells (Figure 1A). There is no FABP3 expression and a very little FABP7 expression in Neuro-2A cells (Figure S1). CCK-8 assays revealed that rotenone at concentrations $> 1 \mu\text{M}$ significantly decreased cell viability in mock- and FABP5-transfected cells (Figure 1B). Similar toxicity of oxidative stress was demonstrated in α Syn-transfected cells, whereas above 0.5 μM , rotenone treatment further decreased cell viability in α Syn/FABP5 (α S/F5)-expressing cells (Figure 1C). This effect of rotenone was evident when treated at a moderate concentration (0.5 μM), which failed to decrease cell survival in α Syn-transfected cells. These results suggested that FABP5 enhances oxidative stress toxicity in the presence of α Syn.

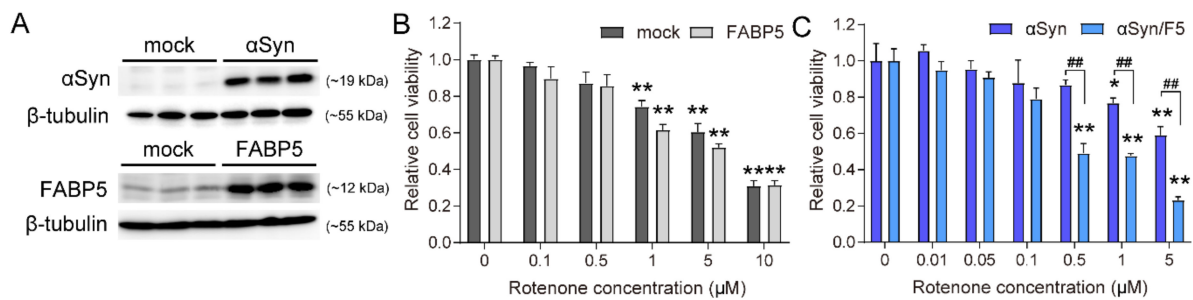


Figure 1. Rotenone induced neurotoxicity, especially with co-overexpression of FABP5 and α -Synuclein. (A) Representative images of immunoblots probed with antibodies against α Syn (~19 kDa) and FABP5 (~12 kDa). Blots with anti- β -tubulin antibody showed that a similar amount of protein was loaded. (B,C) Viability of Neuro-2A cells treated with indicated concentrations of rotenone for 48 h was assessed using CCK-8 assays. The transfection conditions were pcDNA 3.1-transfected cells (mock) and FABP5-transfected cells in (B); α Syn-transfected cells and α Syn/FABP5-transfected cells (α S/F5) in (C). Results are presented as means \pm SEM (n = 4 parallel cell experiments). * $p < 0.05$, ** $p < 0.01$, vs. 0 μ M rotenone groups; ## $p < 0.01$ vs. α Syn-transfected cells. CCK-8: cell counting kit-8.

3.2. Rotenone Induces α -Synuclein and FABP5 Oligomerization and Aggregation

We next asked whether the toxicity of rotenone is associated with α Syn oligomerization or aggregation. We separated cell lysates into Triton-soluble and SDS-soluble fractions, as evaluated by immunoblotting under non-denatured conditions (Figure 2). α Syn and FABP5 monomers remained in the Triton-soluble fractions (Figure 2A,C). Meanwhile, the levels of α Syn oligomers (70–140 kDa) and aggregates (>210 kDa) significantly increased following 0.1 μ M rotenone treatment (Figure 2B,F,G). α Syn dimer/trimer levels were also upregulated, but this difference was not statistically significant (Figure 2E). Furthermore, immunoblotting analysis with α Syn antibody and re-blotting with FABP5 antibody showed that there were also oligomers and aggregates at the same molecular weights as α Syn (Figure 2D). Quantitative analysis revealed upregulation of dimer/trimer (30–55 kDa), oligomers (70–140 kDa), and aggregates (>210 kDa) in rotenone-treated cells, but there was a statistically significant difference only in term of aggregate levels (Figure 2E–G). The negative control of immunoblotting was shown in Figure S2, and there is no target band detected. These results suggested that FABP5 cooperates with α Syn oligomerization and aggregation under oxidative stress.

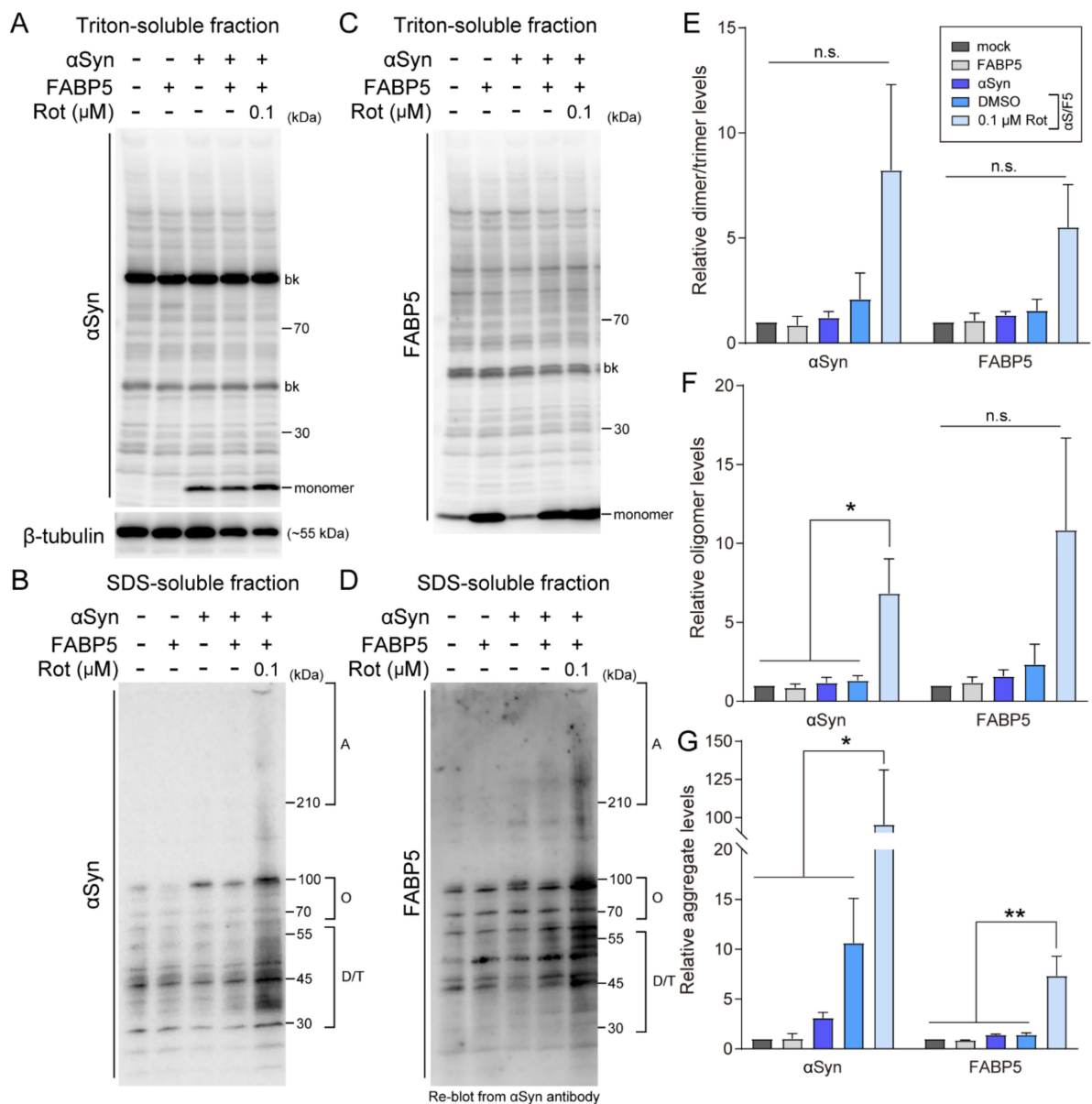


Figure 2. Effects of rotenone on α Syn oligomerization and aggregation in FABP5/ α Syn-transfected Neuro-2A cells. (A–D) Representative images of immunoblots probed with antibodies against α Syn and FABP5 under non-denaturing conditions of Triton-soluble and SDS-soluble fractions. Detection with anti- β -tubulin antibody was used as a protein-loading control. (E–G) Quantitative analyses of protein contents of different molecular weights, which indicate protein complexes of dimer/trimers, oligomers, and aggregates. Results are presented as means \pm SEM ($n = 3$ respective cell experiments). * $p < 0.05$, ** $p < 0.01$, vs. 0.1 μ M rotenone-treated α S/F5 cells. n.s., not statistically significant. D/T: dimers/trimers; O: oligomers; A: aggregates. bk besides blots indicate non-specific bands.

3.3. FABP5 Co-Localizes with α Syn Aggregates Induced by Oxidative Stress

Next, cells were subjected to immunofluorescent staining to analyze the subcellular localization of α Syn and FABP5 (Figure 3). The signals detected for both α Syn and FABP5 showed a diffused cellular pattern of localization (Figure 3A). However, when treated with 0.1 or 0.5 μ M rotenone, immunolabeling revealed visible significant α Syn accumulation in FABP5/ α Syn co-overexpressing cells (Figure 3B, arrow). FABP5 immunoreactivity co-localized with α Syn aggregates in rotenone-treated cells (Figure 3B), suggesting that FABP5 forms complexes with α Syn aggregates. Taken together, these results suggested

that rotenone promotes FABP5 and α Syn interactions, thereby causing α Syn oligomer and aggregate formation.

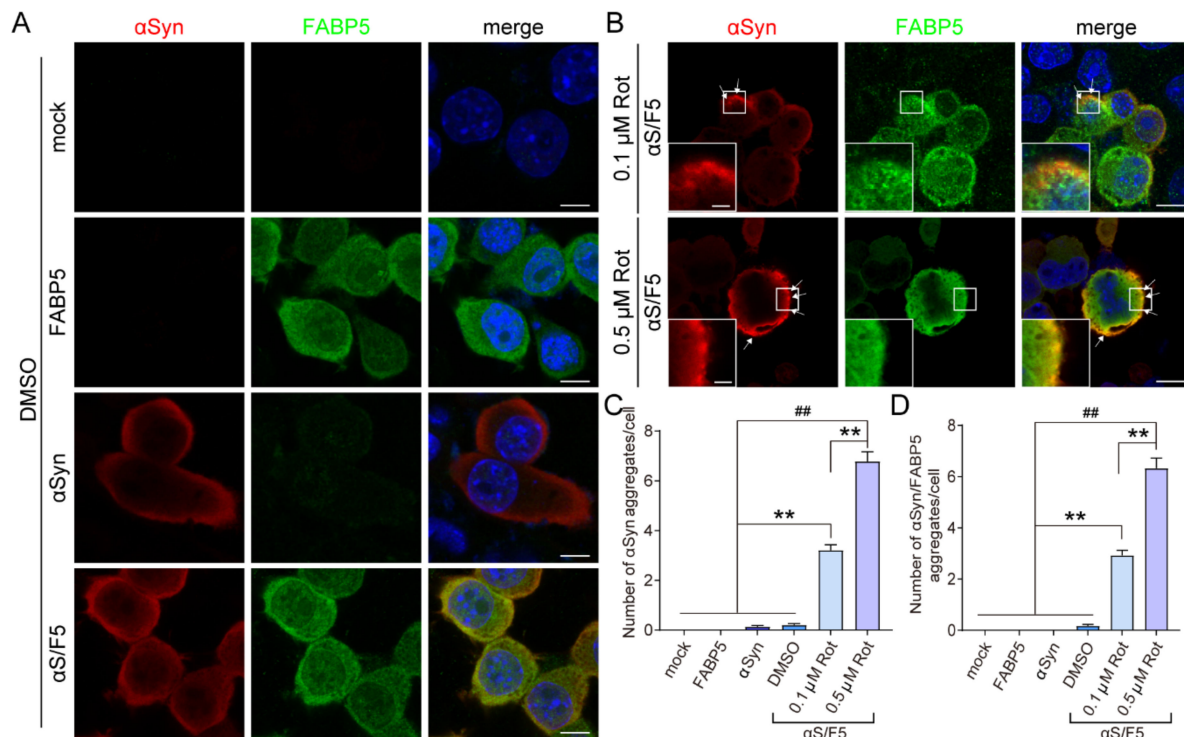


Figure 3. FABP5 co-localized with rotenone-induced α -Synuclein aggregates. **(A,B)** Representative images of immunofluorescent staining showing localization of α Syn (red), FABP5 (green), and DAPI (blue) in Neuro-2A cells. **(A)** Cells were transfected with pcDNA 3.1, *FABP5*, *α Syn*, and *α S/F5* respectively, then exposed to DMSO. Scale bars: 10 μ m. **(B)** *α S/F5*-transfected cells were exposed to 0.1 or 0.5 μ M rotenone. Arrows indicate α Syn aggregates in cells treated with rotenone. Scale bars: 10 μ m. The region of interest is indicated with a white square and magnified in insets. Scale bars in the higher magnifying images: 2 μ m. **(C,D)** Quantitative analyses of the numbers of α Syn aggregates and α Syn/FABP5 positive aggregates. Results are presented as means \pm SEM ($n > 40$ cells from three respective cell experiments). ** $p < 0.01$, vs. 0.1 μ M rotenone-treated *α S/F5* cells; ## $p < 0.01$, vs. 0.5 μ M rotenone-treated *α S/F5* cells.

3.4. FABP5 is Involved in Mitochondrial Membrane Potential Reduction by Rotenone

We further employed the JC-1 assay to detect mitochondrial membrane potentials (Figure 4). Reductions in mitochondrial membrane potentials are indicated by a decrease in the ratio of red to green fluorescence of the JC-1 dye. First, we evaluated the effects of transfection on cells and found that there were no obvious effects (Figure 4A,C). Meanwhile, treatment with rotenone at 0.1 and 0.5 μ M significantly decreased JC-1 red fluorescence and the ratio (red/green), especially in *α Syn/F5* cells (Figure 4B,D). The ratio at 0.1 μ M rotenone was not altered in *α Syn*-expressing cells, but was significantly reduced in *α Syn/F5* cells (Figure 4D).

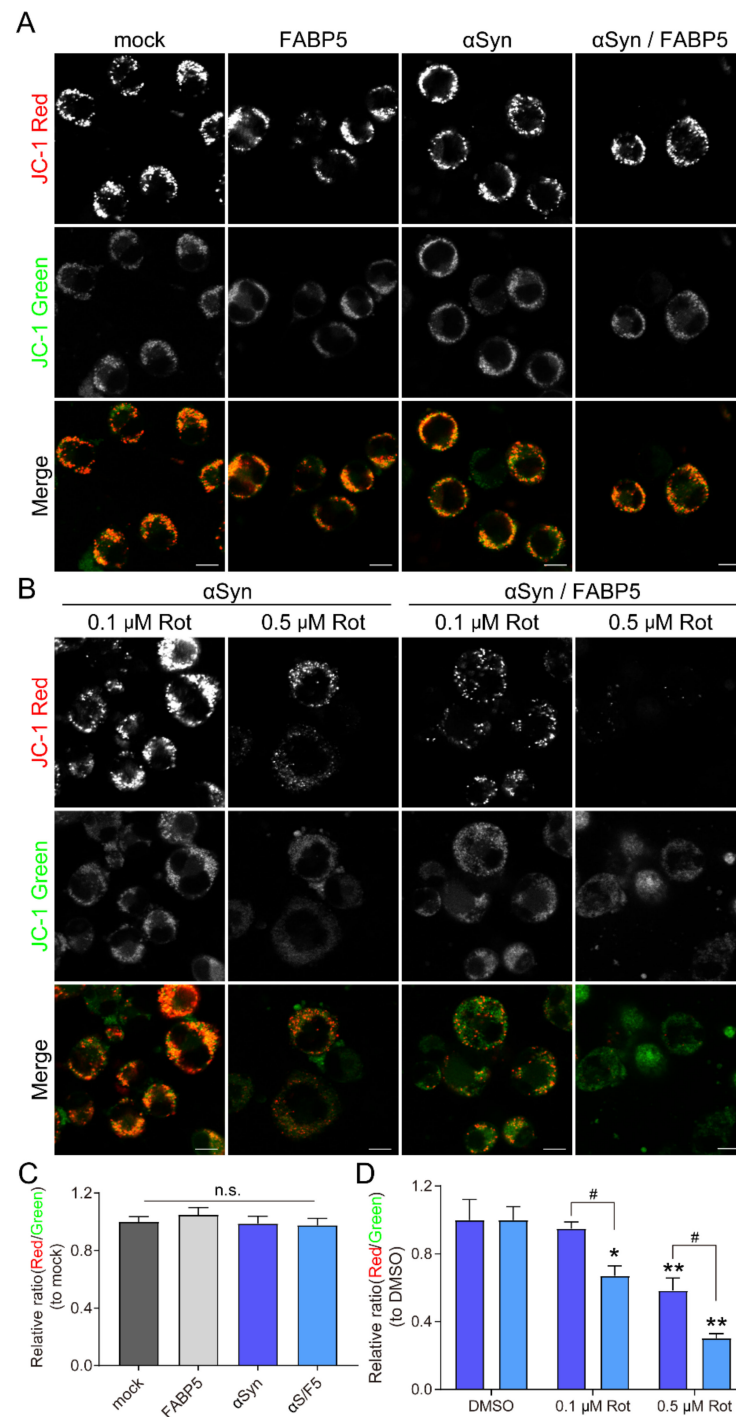


Figure 4. FABP5 involvement in rotenone-induced reduction of mitochondrial activity. **(A,B)** Representative images of JC-1-stained Neuro-2A cells. The decrease in the ratio of red to green fluorescence of JC-1 dye was indicated by a reduction in mitochondrial membrane potential. **(A)** Cells were transfected with pcDNA 3.1, *FABP5*, *α Syn*, and *α S/F5*, respectively, then exposed to DMSO. **(B)** *α Syn* and *α S/F5* transfected cells were exposed to 0.1 or 0.5 μ M rotenone. **(C,D)** Graphs demonstrating the quantification of the ratio of JC-1 red to green fluorescent intensity in Neuro-2A cells. Results are presented as means \pm SEM ($n > 300$ cells in C and $n = 5$ wells in D from parallel cell experiments). * $p < 0.05$, ** $p < 0.01$, vs. DMSO-treated groups; # $p < 0.05$, vs. *α Syn*-transfected groups. n.s., not statistically significant. Scale bars: 10 μ m.

3.5. FABP5 Ligand Rescues Rotenone-Induced Cell Death and Impedes α Syn Oligomerization and Aggregation

Next, we evaluated whether FABP5 ligand can abolish oxidative stress toxicity and α Syn oligomerization. BMS309403 was identified as a small-molecule FABP4-selective inhibitor, with a particularly high affinity for FABP4 [27]. Previously, we developed several BMS309403 derivatives and reported their affinity for GST-FABP5 [24,28]. Based on these studies, we used ligand 7, which has high affinity for FABP5, with a dissociation constant (K_d) of 199 ± 23 nM, which is almost identical to that of the intrinsic fatty acid, arachidonic acid (AA) at 228 ± 43 nM (Figure 5A,B) [24]. Treatment of ligand 7 increased cell viability after 0.5 μ M rotenone treatment, and there was a statistically significant difference at 1 and 3 μ M ligand 7 (Figure 5C). The reduction in the JC-1 ratio (red/green) by rotenone was also significantly improved by treatment with 1 μ M ligand 7 (Figure 5D). We further analyzed oligomerization and aggregation of α Syn and FABP5 in the SDS-soluble fraction, which was apparently suppressed by ligand 7 (Figure 5E,F). At the same time, the monomers of α Syn and FABP5 remained in Triton-soluble fractions, which is consistent with Figure 2A,C and Figure 5G. These results suggested that FABP5 inhibitor (ligand 7) effectively attenuated α Syn oligomerization and toxicity by conserving mitochondrial function.

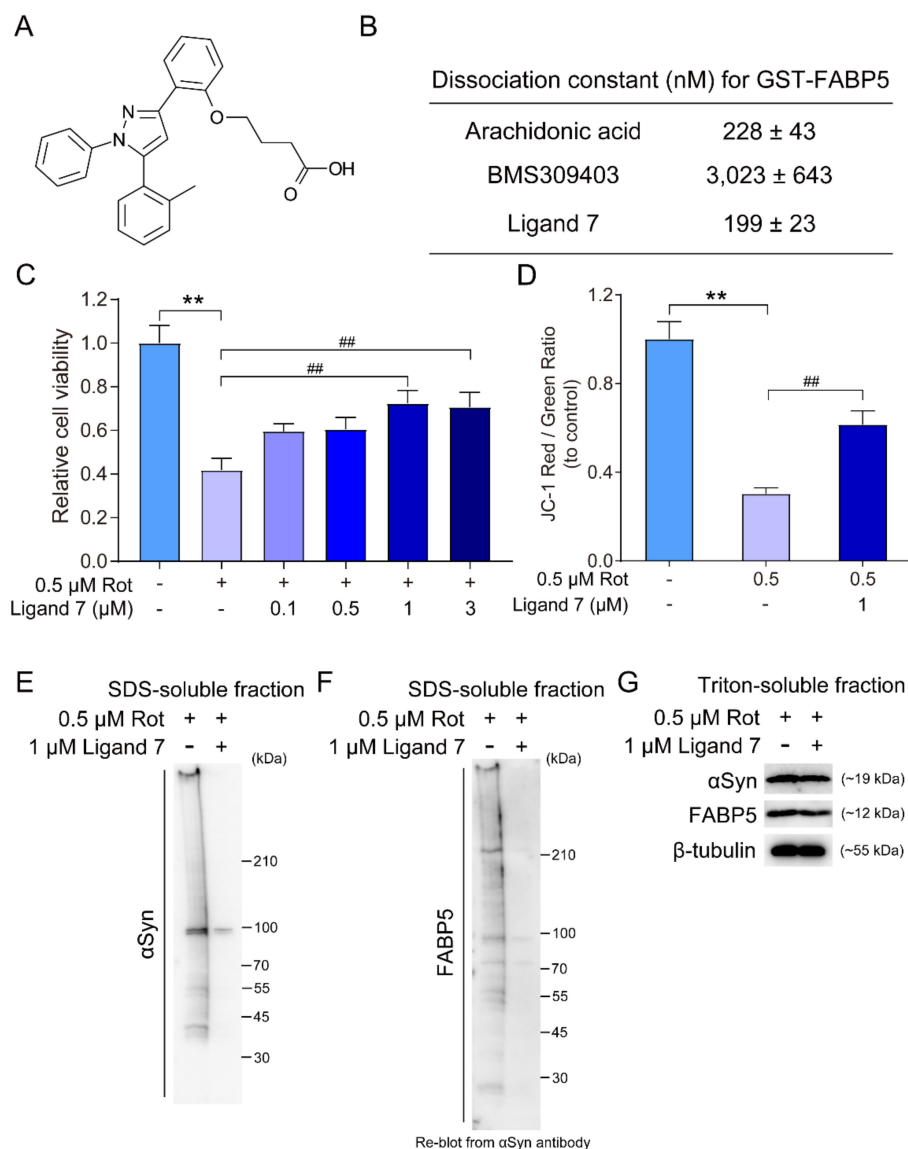


Figure 5. Effects of FABP5 ligand 7 on cell death and α Syn oligomerization and aggregation. All experiments in Figure 5 were carried in α S/F5-transfected cells. (A) Chemical structure of ligand 7. (B) Dissociation constants (K_d values, nM) of arachidonic acid, BMS309403, and ligand 7 for GST-FABP5 [24]. (C) α S/F5-transfected cells were exposed to 0.5 μ M rotenone and the indicated concentrations of ligand 7 for 48 h. Cell viability was measured using CCK-8 assays. Results are presented as means \pm SEM ($n = 6$ parallel cell experiments). ** $p < 0.01$, vs. non-rotenone-treated cells; ## $p < 0.01$, vs. rotenone-treated cells without ligand. (D) Graphs demonstrating quantification of the JC-1 ratio (red/green). Results are presented as means \pm SEM ($n = 5$ parallel cell experiments). ** $p < 0.01$, vs. non-rotenone-treated cells; ## $p < 0.01$, vs. rotenone-treated cells without ligand. (E,F) Representative images of immunoblots developed with antibodies against α Syn and FABP5 in α S/F5 cells treated with ligand 7. Three parallel cell experiments were performed with similar results. (G) The monomers of α Syn and FABP5 remain in Triton-soluble fractions. Incubation with β -tubulin antibody was used as a protein-loading control.

3.6. FABP5/ α Syn Aggregates Targeting Mitochondria and Ligand 7 Prevent Abnormal Accumulation

To further evaluate the mechanisms involved in protection, we isolated mitochondria from α Syn/F5 cells (Figure 6A). Crude mitochondrial and cytosolic fractions were separated and subjected to immunoblotting assays (Figure 6B,C). As a result, FABP5 and α Syn abnormally accumulated in mitochondria in 0.5 μ M rotenone-treated cells, which was

prevented by 1 μM ligand 7 treatment (Figure 6D,E). Consistent with these immunoblotting results, αSyn and FABP5 were co-localized with the mitochondrial marker MitoTracker in rotenone-treated cells (Figure 6F, arrow), which was blocked by ligand 7 treatment (Figure 6F).

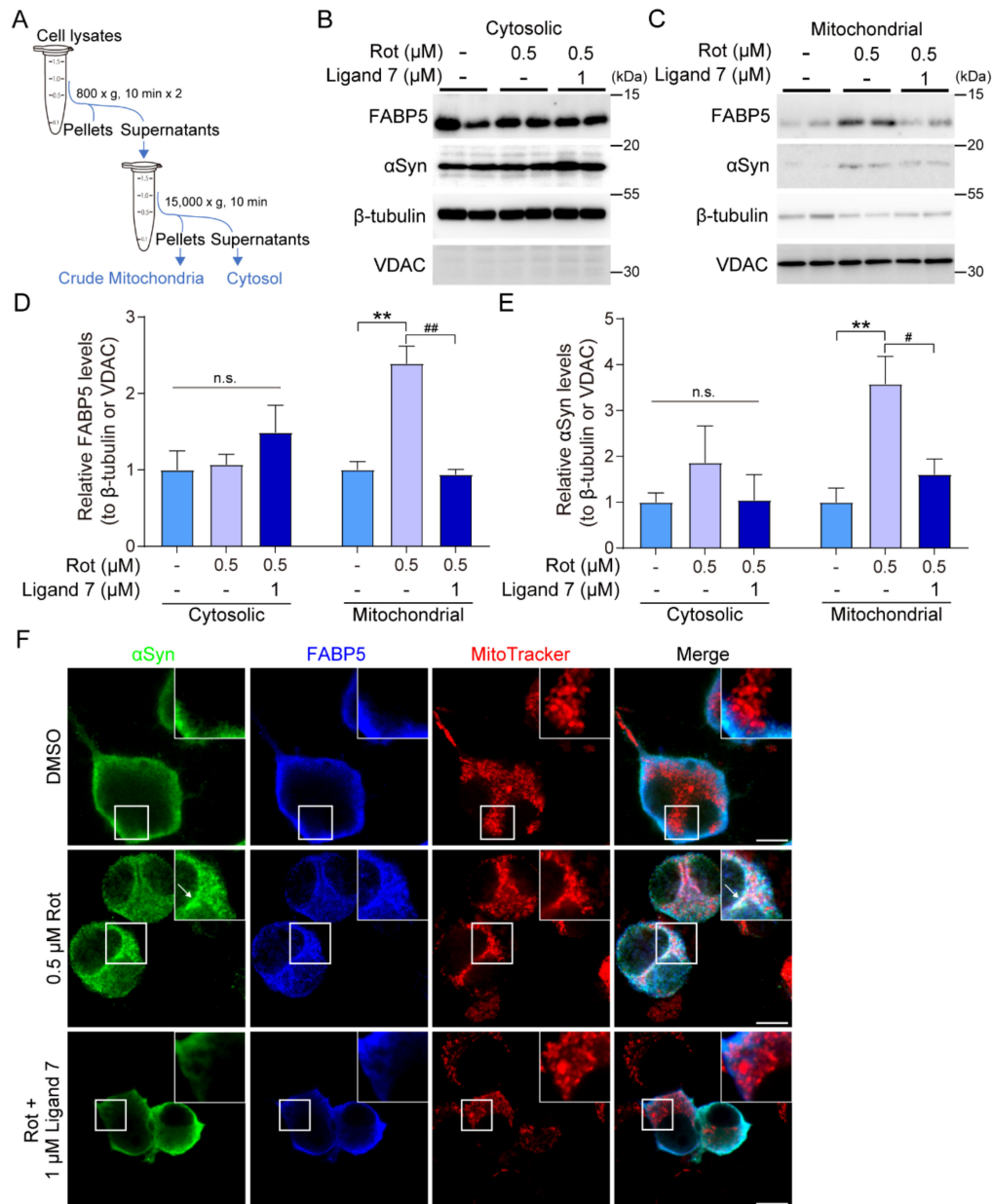


Figure 6. Abnormal accumulation of FABP5 and αSyn in mitochondria was prevented by ligand 7 treatment. All experiments were carried in $\alpha\text{S}/\text{F5}$ -transfected cells. (A) Simple diagram of the mitochondrial isolation process in $\alpha\text{S}/\text{F5}$ -transfected cells. (B,C) Representative images of immunoblots probed with antibodies against FABP5 and αSyn . Incubation with anti- β -tubulin or VDAC antibodies were used as protein-loading controls for cytosolic or mitochondrial fractions, respectively. (D,E) Quantitative densitometric analyses of αSyn and FABP5 in different fractions. Results are presented as means \pm SEM ($n = 4$, two respective cell experiments, each with 2 parallel dishes). ** $p < 0.01$, vs. non-rotenone-treated cells; # $p < 0.05$ and ## $p < 0.01$, 1 μM vs. rotenone-treated cells without ligand. (F) Confocal images of αSyn (green), FABP5 (blue), and MitoTracker (red) in $\alpha\text{S}/\text{F5}$ -transfected cells. The region of interest is indicated with a white square and magnified in insets. Arrow indicates αSyn aggregates which approach and gather in mitochondria with FABP5 in rotenone-treated cells. There were no significant αSyn - and FABP5-positive aggregates in mitochondria of ligand 7-treated cells. Scale bars: 10 μm .

4. Discussion

In this study, we demonstrated that FABP5 plays a key role in oligomerization and aggregation of α Syn under oxidative stress in Neuro-2A cells. In the absence of rotenone, both α Syn and FABP5 localized with diffuse patterns in these cells (Figure 3A); however, their aggregates appeared concentration-dependent on rotenone (Figure 3B–D). Rotenone also led to aggregate localization in mitochondria, and decreased mitochondrial membrane potential, which might have resulted in cell death (Figure 7). We also found that FABP5 ligand 7 treatment abolished the toxicity, α Syn aggregation, and mitochondrial impairment in Neuro-2A cells.

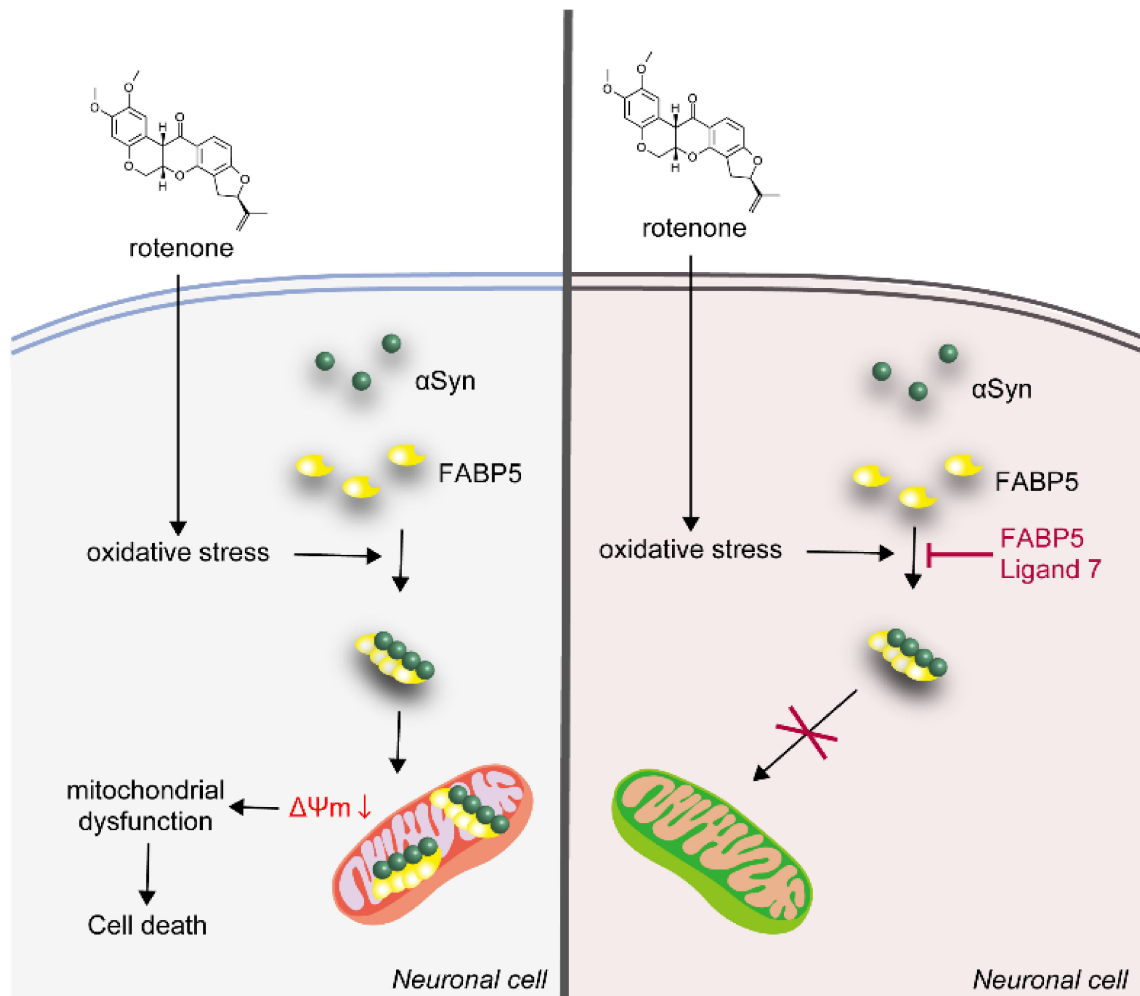


Figure 7. Schematic diagram of the mechanism by which α Syn/FABP5 aggregates aggravate mitochondrial dysfunction and induce neuronal cell apoptosis. FABP5 ligand 7 binds with FABP5 and blocks aggregate formation to attenuate neurotoxicity. **(Left)** when exposed to rotenone, α Syn accumulated with FABP5 to form oligomers and aggregates, which were further targeted to mitochondria. The reduced mitochondrial membrane potential indicated mitochondrial dysfunction which induced cell death. **(Right)** pharmacological inhibition of FABP5 by ligand 7 prevented α Syn/FABP5 aggregate formation, thereby rescuing neuronal cells.

The most basic function of FABPs is to participate in the utilization of lipids in food-stuffs, and to mediate fatty acid transport to various organelles, including mitochondria. A recent study indicated that both acute shRNA knockdown of FABP5 and pharmacologic inhibition results in decreased mitochondrial mass and respiration in regulatory T cells [29]. FABP5 induces mitochondrial macropore formation through BAX and voltage-dependent anion channels (VDAC-1), which mediate mitochondrial outer membrane permeabiliza-

tion and ultimately accelerates mitochondria-induced oligodendrocyte death. However, FABP7 does not localize in mitochondria under mitochondrial damage [30]. In FABP3-overexpressing embryonic cancer cells (P19 cells), lower cellular ATP production was accompanied by a dramatic decrease in mitochondrial membrane potential, and FABP3 overexpression also led to an imbalance in mitochondrial dynamics and excess intracellular reactive oxygen species production [31]. These studies suggest that FABP proteins regulate mitochondrial function by transporting fatty acids and reactive oxygen species production in cells. In this study, however, we failed to confirm the changes to mitochondrial membrane potential by FABP5 overexpression alone (Figure 4).

Various stimuli, including oxidative stress, can trigger translocation of α Syn to the mitochondria. Transient or stable transfection of α Syn particles exhibit localization in the mitochondria of neuroblastoma SHSY or HEK293 cells [32,33]. Expression of α Syn induces cytochrome C release from mitochondria, or vulnerability to rotenone in these cultured cells. Cellular acidification is also reported to enhance mitochondrial α Syn accumulation [34]. In this study, we could not confirm α Syn localization to mitochondria, or upregulated toxicity of rotenone by overexpression of α Syn alone. Oxidative stress induced by rotenone triggered toxicity and α Syn oligomerization and mitochondrial injury was aggravated by FABP5 co-expressed in Neuro-2A cells (Figure 6).

Aggregation and mitochondrial localization of α Syn and FABP5 may underlie the toxic mechanisms induced by rotenone. Reactive oxygen species produce oxidized aldehydes of polyunsaturated fatty acids such as 4-hydroxy-2-nonenal (4-HNE), 4-hydroxy-2-hexenal, and malondialdehyde [35]. FABP4, another FABP family protein, binds not only with fatty acids, but also with metabolites such as 4-HNE [36]. Fatty acids are usually located in the internal pocket of FABPs; however, 4-HNE can undergo covalent binding with a cysteine residue at amino acid 117. This suggests that strong modifications of FABP protein leads to prolonged regulation of its function. Such modification may underlie mechanisms involving FABP5 localization together with α Syn in mitochondria, because this cysteine residue is also conserved in FABP5, and ligand 7 treatment inhibited aggregation and mitochondrial localization (Figure 6) [24]. However, further studies are required to evaluate the underlying mechanisms whereby FABP5 and α Syn aggregations localize to mitochondria.

Finally, we investigated whether FABP5 ligand treatment prevented its aggregation and localization with α Syn induced by rotenone. FABP5 is highly expressed in the dopaminergic neurons of SNpc [23]; however, little is known regarding the physiological relevance in the neurons or pathological roles of FABP5 in PD. Our study provides evidence that FABP5 protein is a potential therapeutic target in PD therapy.

Supplementary Materials: The following are available online at <https://www.mdpi.com/2227-9059/9/2/110/s1>, Figure S1: There is no FABP3 and a very little FABP7 expression in Neuro-2A cells (mock cells), Figure S2: The negative control of immunoblotting assay.

Author Contributions: Y.W.: investigation and original draft writing; Y.S. and A.C.: investigation; I.K.: methodology, K.F.: supervision, review/editing, project administration, and funding. All authors have read and agreed to the published version of the manuscript.

Funding: This work was supported in part by the Strategic Research Program for Brain Sciences from the Japan Agency for Medical Research and Development (JP19dm0107071 and JP20dm0107071; awarded to K.F.

Data Availability Statement: The data presented in this study are available on request from the corresponding author.

Conflicts of Interest: The authors declare no conflict of interest.

References

1. Fields, C.R.; Bengoa-Vergniory, N.; Wade-Martins, R. Targeting Alpha-Synuclein as a Therapy for Parkinson's Disease. *Front. Mol. Neurosci.* **2019**, *12*, 299. [[CrossRef](#)] [[PubMed](#)]
2. Mhyre, T.R.; Boyd, J.T.; Hamill, R.W.; Maguire-Zeiss, K.A. Parkinson's disease. *Subcell. Biochem.* **2012**, *65*, 389–455. [[CrossRef](#)] [[PubMed](#)]
3. Spillantini, M.G.; Schmidt, M.L.; Lee, V.M.Y.; Trojanowski, J.Q.; Jakes, R.; Goedert, M. α -synuclein in Lewy bodies. *Nature* **1997**, *388*, 839–840. [[CrossRef](#)]
4. Gilmozzi, V.; Gentile, G.; Castelo Rueda, M.P.; Hicks, A.A.; Pramstaller, P.P.; Zanon, A.; Lévesque, M.; Pichler, I. Interaction of Alpha-Synuclein With Lipids: Mitochondrial Cardiolipin as a Critical Player in the Pathogenesis of Parkinson's Disease. *Front. Neurosci.* **2020**, *14*, 1051. [[CrossRef](#)]
5. Villar-Piqué, A.; Lopes da Fonseca, T.; Outeiro, T.F. Structure, function and toxicity of alpha-synuclein: The Bermuda triangle in synucleinopathies. *J. Neurochem.* **2016**, *139*, 240–255. [[CrossRef](#)]
6. Bengoa-Vergniory, N.; Roberts, R.F.; Wade-Martins, R.; Alegre-Abarategui, J. Alpha-synuclein oligomers: A new hope. *Acta Neuropathol.* **2017**, *134*, 819–838. [[CrossRef](#)]
7. Delenclos, M.; Burgess, J.D.; Lamprokostopoulou, A.; Outeiro, T.F.; Vekrellis, K.; McLean, P.J. Cellular models of alpha-synuclein toxicity and aggregation. *J. Neurochem.* **2019**, *150*, 566–576. [[CrossRef](#)]
8. Kalia, L.V.; Kalia, S.K.; Lang, A.E. Disease-modifying strategies for Parkinson's disease. *Mov. Disord.* **2015**, *30*, 1442–1450. [[CrossRef](#)] [[PubMed](#)]
9. Rodríguez-Losada, N.; de la Rosa, J.; Larriva, M.; Wendelbo, R.; Aguirre, J.A.; Castresana, J.S.; Ballaz, S.J. Overexpression of alpha-synuclein promotes both cell proliferation and cell toxicity in human SH-SY5Y neuroblastoma cells. *J. Adv. Res.* **2020**, *23*, 37–45. [[CrossRef](#)]
10. Davis, G.C.; Williams, A.C.; Markey, S.P.; Ebert, M.H.; Caine, E.D.; Reichert, C.M.; Kopin, I.J. Chronic parkinsonism secondary to intravenous injection of meperidine analogues. *Psychiatry Res.* **1979**, *1*, 249–254. [[CrossRef](#)]
11. Ramsay, R.R.; Salach, J.I.; Singer, T.P. Uptake of the neurotoxin 1-methyl-4-phenylpyridine (MPP⁺) by mitochondria and its relation to the inhibition of the mitochondrial oxidation of NAD⁺-linked substrates by MPP⁺. *Biochem. Biophys. Res. Commun.* **1986**, *134*, 743–748. [[CrossRef](#)]
12. Schapira, A.H.V.; Gegg, M. Mitochondrial contribution to parkinson's disease pathogenesis. *Parkinsons. Dis.* **2011**, *2011*, 159160. [[CrossRef](#)] [[PubMed](#)]
13. Grassi, D.; Howard, S.; Zhou, M.; Diaz-Perez, N.; Urban, N.T.; Guerrero-Given, D.; Kamasawa, N.; Volpicelli-Daley, L.A.; LoGrasso, P.; Lasmézas, C.I. Identification of a highly neurotoxic α -synuclein species inducing mitochondrial damage and mitophagy in Parkinson's disease. *Proc. Natl. Acad. Sci. USA* **2018**, *115*, E2634–E2643. [[CrossRef](#)] [[PubMed](#)]
14. Di Maio, R.; Barrett, P.J.; Hoffman, E.K.; Barrett, C.W.; Zharikov, A.; Borah, A.; Hu, X.; McCoy, J.; Chu, C.T.; Burton, E.A.; et al. α -synuclein binds to TOM20 and inhibits mitochondrial protein import in Parkinson's disease. *Sci. Transl. Med.* **2016**, *8*, 1–15. [[CrossRef](#)] [[PubMed](#)]
15. Nakamura, K.; Nemani, V.M.; Azarbal, F.; Skibinski, G.; Levy, J.M.; Egami, K.; Munishkina, L.; Zhang, J.; Gardner, B.; Wakabayashi, J.; et al. Direct membrane association drives mitochondrial fission by the Parkinson disease-associated protein α -synuclein. *J. Biol. Chem.* **2011**, *286*, 20710–20726. [[CrossRef](#)] [[PubMed](#)]
16. Li, B.; Hao, J.; Zeng, J.; Sauter, E.R. SnapShot: FABP Functions. *Cell* **2020**, *182*, 1066. [[CrossRef](#)] [[PubMed](#)]
17. Furuhashi, M.; Hotamisligil, G.S. Fatty acid-binding proteins: Role in metabolic diseases and potential as drug targets. *Nat. Rev. Drug Discov.* **2008**, *7*, 489–503. [[CrossRef](#)]
18. D'Anneo, A.; Bavisotto, C.C.; Gammazza, A.M.; Paladino, L.; Carlisi, D.; Cappello, F.; de Macario, E.C.; Macario, A.J.L.; Lauricella, M. Lipid chaperones and associated diseases: A group of chaperonopathies defining a new nosological entity with implications for medical research and practice. *Cell Stress Chaperones* **2020**, *25*, 805–820. [[CrossRef](#)]
19. Bando, Y.; Yamamoto, M.; Sakiyama, K.; Inoue, K.; Takizawa, S.; Owada, Y.; Iseki, S.; Kondo, H.; Amano, O. Expression of epidermal fatty acid binding protein (E-FABP) in septoclasts in the growth plate cartilage of mice. *J. Mol. Histol.* **2014**, *45*, 507–518. [[CrossRef](#)]
20. Yu, S.; Levi, L.; Casadesus, G.; Kunos, G.; Noy, N. Fatty acid-binding protein 5 (fabp5) regulates cognitive function both by decreasing anandamide levels and by activating the nuclear receptor peroxisome proliferator-activated receptor α/β (ppar α/β) in the brain. *J. Biol. Chem.* **2014**, *289*, 12748–12758. [[CrossRef](#)]
21. Owada, Y.; Yoshimoto, T.; Kondo, H. Spatio-temporally differential expression of genes for three members of fatty acid binding proteins in developing and mature rat brains. *J. Chem. Neuroanat.* **1996**, *12*, 113–122. [[CrossRef](#)]
22. Liu, R.Z.; Mita, R.; Beaulieu, M.; Gao, Z.; Godbout, R. Fatty acid binding proteins in brain development and disease. *Int. J. Dev. Biol.* **2010**, *54*, 1229–1239. [[CrossRef](#)] [[PubMed](#)]
23. Zhou, Q.; Li, J.; Wang, H.; Yin, Y.; Zhou, J. Identification of nigral dopaminergic neuron-enriched genes in adult rats. *Neurobiol. Aging* **2011**, *32*, 313–326. [[CrossRef](#)] [[PubMed](#)]
24. Shinoda, Y.; Wang, Y.; Yamamoto, T.; Miyachi, H.; Fukunaga, K. Analysis of binding affinity and docking of novel fatty acid-binding protein (FABP) ligands. *J. Pharmacol. Sci.* **2020**, *143*, 264–271. [[CrossRef](#)]
25. Schneider, C.A.; Rasband, W.S.; Eliceiri, K.W. NIH Image to ImageJ: 25 years of image analysis. *Nat. Methods* **2012**, *9*, 671–675. [[CrossRef](#)]

26. Carré, M.; André, N.; Carles, G.; Borghi, H.; Brichese, L.; Briand, C.; Braguer, D.; Medicine, U.F.R.; La, U.O. Tubulin is an inherent component of mitochondrial membranes that interacts with the voltage-dependent anion channel. *J. Biol. Chem.* **2002**, *277*, 33664–33669. [[CrossRef](#)]
27. Sulsky, R.; Magnin, D.R.; Huang, Y.; Simpkins, L.; Taunk, P.; Patel, M.; Zhu, Y.; Stouch, T.R.; Bassolino-Klimas, D.; Parker, R.; et al. Potent and selective biphenyl azole inhibitors of adipocyte fatty acid binding protein (aFABP). *Bioorg. Med. Chem. Lett.* **2007**, *17*, 3511–3515. [[CrossRef](#)]
28. Cheng, A.; Shinoda, Y.; Yamamoto, T.; Miyachi, H.; Fukunaga, K. Development of FABP3 ligands that inhibit arachidonic acid-induced α -synuclein oligomerization. *Brain Res.* **2019**, *1707*, 190–197. [[CrossRef](#)]
29. Field, C.S.; Baixauli, F.; Kyle, R.L.; Puleston, D.J.; Cameron, A.M.; Sanin, D.E.; Hippen, K.L.; Loschi, M.; Thangavelu, G.; Corrado, M.; et al. Mitochondrial Integrity Regulated by Lipid Metabolism Is a Cell-Intrinsic Checkpoint for Treg Suppressive Function. *Cell Metab.* **2020**, *31*, 422–437. [[CrossRef](#)]
30. Cheng, A.; Kawahata, I.; Fukunaga, K. Fatty acid binding protein 5 mediates cell death by psychosine exposure through mitochondrial macropores formation in oligodendrocytes. *Biomedicines* **2020**, *8*, 635. [[CrossRef](#)]
31. Song, G.X.; Shen, Y.H.; Liu, Y.Q.; Sun, W.; Miao, L.P.; Zhou, L.J.; Liu, H.L.; Yang, R.; Kong, X.Q.; Cao, K.J.; et al. Overexpression of FABP3 promotes apoptosis through inducing mitochondrial impairment in embryonic cancer cells. *J. Cell. Biochem.* **2012**, *113*, 3701–3708. [[CrossRef](#)] [[PubMed](#)]
32. Parihar, M.S.; Parihar, A.; Fujita, M.; Hashimoto, M.; Ghafourifar, P. Mitochondrial association of alpha-synuclein causes oxidative stress. *Cell. Mol. Life Sci.* **2008**, *65*, 1272–1284. [[CrossRef](#)] [[PubMed](#)]
33. Shavali, S.; Brown-Borg, H.M.; Ebadi, M.; Porter, J. Mitochondrial localization of alpha-synuclein protein in alpha-synuclein overexpressing cells. *Neurosci. Lett.* **2008**, *439*, 125–128. [[CrossRef](#)] [[PubMed](#)]
34. Cole, N.B.; DiEuliis, D.; Leo, P.; Mitchell, D.C.; Nussbaum, R.L. Mitochondrial translocation of α -synuclein is promoted by intracellular acidification. *Exp. Cell Res.* **2008**, *314*, 2076–2089. [[CrossRef](#)]
35. Assies, J.; Mocking, R.J.T.; Lok, A.; Ruhé, H.G.; Pouwer, F.; Schene, A.H. Effects of oxidative stress on fatty acid- and one-carbon-metabolism in psychiatric and cardiovascular disease comorbidity. *Acta Psychiatr. Scand.* **2014**, *130*, 163–180. [[CrossRef](#)]
36. Hellberg, K.; Grimsrud, P.A.; Kruse, A.C.; Banaszak, L.J.; Ohlendorf, D.H.; Bernlohr, D.A. X-ray crystallographic analysis of adipocyte fatty acid binding protein (aP2) modified with 4-hydroxy-2-nonenal. *Protein Sci.* **2010**, *19*, 1480–1489. [[CrossRef](#)]